J. Ocean Univ. China (Oceanic and Coastal Sea Research)
https://doi.org/10.1007/s11802-025-5929-5
ISSN 1672-5182, 2025 24 (2): 427-438
http://www.ouc.edu.cn/xbywb/
E-mail:xbywb@ouc.edu.cn

Genome-Wide Analysis of Urea Transporter (*ut*) Gene Family in Spotted Sea Bass (*Lateolabrax maculatus*): Evolution and Differential Expression After Salinity Adaptation

YANG Rutao[1)], HUANG Zurui[2)], LI Jinku[1)], WEN Haishen[1)], QI Xin[1)], ZHANG Kaiqiang[1)], ZHANG Jingru[1)], LIU Mengqun[1)], LI Jifang[1)], ZHANG Meizhao[1)], and LI Yun[1), *]

1) *Key Laboratory of Mariculture*, *Ministry of Education (KLMME)*, *Ocean University of China*, *Qingdao* 266003, *China*
2) *National Genomics Data Center*, *Beijing Institute of Genomics*, *Chinese Academy of Sciences and China National Center for Bioinformation*, *Beijing* 100101, *China*

(Received March 3, 2024; revised June 27, 2024; accepted September 24, 2024)

Abstract Urea is a major end product of nitrogen catabolism, serving as an osmolyte to regulate osmotic stress in fish exposed to varying water environments. It has been well known that urea transporters (UTs) facilitate the rapid movement of urea across cell membranes. However, researches on *ut* genes were predominantly focused on elasmobranchs and early developmental stages of fish. In this investigation, a total of three *ut* genes were identified in spotted sea bass. Phylogenetic, homology, and syntenic analyses were conducted to validate the annotation and assess the evolutionary relationships among *ut* genes. Both *ut-a* and *ut-b* genes have retained their evolutionary stability, demonstrating a significant level of homology between them. To gain deeper insights into the evolution of *ut* genes in spotted sea bass, we performed selective pressure analysis using site, branch, and branch-site models. The results suggested that positive selection likely played a significant role in shaping the evolution of the *ut* gene family. Furthermore, tissue-specific expression analyses revealed high expression levels of *ut* genes in osmoregulatory tissues such as the gill and kidney. Additionally, all three *ut* genes exhibited salinity-related expression patterns in gill and kidney tissues during both seawater-to-freshwater (SF) and freshwater-to-seawater (FS) adaptation. *In situ* hybridization results demonstrated the localization of both *ut-a* and *ut-c* mRNAs on the gill lamellae and adjacent gill filament epithelium. In summary, our study establishes a solid foundation for future research elucidating the evolutionary relationships and functional significance of *ut* genes during salinity acclimation in spotted sea bass and other teleost species.

Key words spotted sea bass; urea transporter; salinity transfer; gene expression; osmoregulation

1 Introduction

Urea, a major end product of nitrogen catabolism, plays pivotal roles in various metabolic and physiological processes in animals. It serves as a toxic excretory waste product resulting from the detoxification of ammonia, as well as an intermediate product in nitrogen recycling. This recycled urea can be broken down and utilized in the synthesis of amino acids by gut microbes, particularly during hibernation or fasting periods. Additionally, urea functions as an osmolyte to mitigate the osmotic stress induced by high salinity in seawater, a phenomenon commonly observed in fishes (Smith and Wright, 1999). Consequently, the rapid transport of urea is imperative for maintaining osmolality balance amidst fluctuating water environments in fishes (Walsh *et al*., 2000).

Urea transporters (UTs) facilitate the rapid translocation of urea molecules across cell membranes independently of ions such as sodium and chloride (You *et al.*, 1993; Stewart *et al.*, 2005). These UTs are encoded by distinct *ut* genes, including *ut-a*, *ut-b*, and *ut-c*, which belong to the solute carrier 14 (SLC14) family. While *ut-a* and *ut-b* genes are widely distributed in eukaryotes, the *ut-c* gene has thus far been exclusively identified in fishes (Mistry *et al.*, 2005). The first urea transporter was characterized in the kidney of the rabbit (*Oryctolagus cuniculus*) (You *et al.*, 1993). Subsequently, UTs, including their isoforms, have been detected in various tissues of mammals, including red blood cells, kidney, colon, small intestine, cecum, heart, brain, liver, spleen, bone marrow, testis, and lung (Mistry *et al.*, 2001). In mammals, UTs mediate urea transport across erythrocytes (Sands, 1999) and the kidney (Fenton, 2008), facilitating the concentration of urea within the intramedullary collecting duct to maintain high interstitial osmolarity and enhance urine concentration. Furthermore, *ut* genes play a role in the early differentiation of mesenchymal stem cells (MSCs) by modulating osteoblast function and promoting

* Corresponding author. Tel: 0086-532-82031792
E-mail: yunli0116@ouc.edu.cn

adipogenesis (Smith and Wright, 1999; Konno *et al*., 2006; Komrakova *et al.*, 2020). In ruminants, *ut-b* expression is notable in the bovine rumen, where it contributes to the influx of urea into the ruminant digestive tract (Stewart *et al*., 2005).

In non-mammalian vertebrates, cDNAs encoding urea transporters (UTs) have been isolated and characterized from both renal and extrarenal tissues (Couriaud *et al*., 1999; Smith and Wright 1999; Mistry *et al*., 2001, 2005; Hyodo *et al*., 2004; Konno *et al*., 2006). Studies in elasmobranchs and red-eared painted turtles (*Trachemys scripta elegans*) have proposed pivotal roles for *ut* genes in maintaining body fluid homeostasis (Uchiyama *et al*., 2009). During the early developmental stages of teleost, urea transporters are expressed in embryos to facilitate the elimination of urea (Pilley and Wright, 2000), aiding in the detoxification of ammonia accumulated from protein catabolism (Griffith, 1991; Wright *et al*., 1995). In certain teleost species, such as the lake magadi tilapia (*Alcolapia grahami*), *ut* genes fulfill a specialized urea excretion function: UTs are activated periodically throughout the day, translocating urea to the apical surface and inducing the formation of dense-cored vesicles in pavement cells (Laurent *et al*., 2001; Walsh *et al*., 2001). Extensive researches on urea transporters have been focused on osmoregulation in elasmobranchs, including houndshark (*Triakis scyllium*) (Yamaguchi *et al*., 2009), spiny dogfish shark (*Squalus acanthias*) (Smith and Wright, 1999), Atlantic stingray (*Dasyatis Sabina*) (Cabrera *et al*., 2003) and holocephalan elephant fish (*Callorhinchus milii*) (Kakumura *et al*., 2009). Investigations of urea transporters in teleost have also been conducted, and it was found that UTs play a crucial role in ammonia detoxification during the early developmental stages of teleost (Pilley and Wright, 2000), Adult teleost retain specific urea excretion mechanisms and urea transport proteins, and urea excretion comprises only a minor portion of nitrogenous waste, however, the precise role of urea and urea transporters in teleost osmoregulation remains to be fully elucidated.

In fish, urea serves as an important osmotic diuretic to dynamically balance the osmotic pressure of high-salinity seawater, protecting the fish from dehydration and other issues caused by osmotic differences between the body and the external environment (Smith and Wright, 1999). Therefore, urea plays a crucial role in maintaining osmotic balance in fish (Walsh *et al.*, 2000), and its rapid transmembrane transport is primarily mediated by non-ion-dependent urea transporters. It has been reported that the expression of urea transporters in the gills of eels significantly increased during the transition from freshwater to seawater (Mistry *et al.*, 2001). The distribution of urea transporters in the collecting ducts of shark kidneys shows different subcellular patterns under high and low salinities (Yamaguchi *et al.*, 2009). Thus, exploring the physiological functions of urea transporters through salinity adaptation experiments is highly effective.

The spotted sea bass (*Lateolabrax maculatus*) is a euryhaline teleost species along the coast of the northwestern Pacific Ocean. Extensive documentation has shown that spotted sea bass can tolerate a wide range of external salinity environments, ranging from 0 to 45 (Tian *et al*., 2019). Therefore, it serves as an excellent model for identifying *ut* genes and assessing their potential roles in teleost during salinity adaptation. The objective of this study is to investigate the involvement of urea transporters in osmoregulation in teleost, with a particular focus on euryhaline fish.

2 Materials and Methods

2.1 Ethics Statement

All animal experiments were conducted in strict accordance with the guidelines and regulations set forth by the Animal Research and Ethics Committees of Ocean University of China. The research protocol was approved by the respective committees. No endangered or protected species were involved in our study, and all experiments were performed in accordance with the relevant ethical guidelines.

2.2 Genome-Wide Identification of *ut* Genes Family

To identify *ut* genes in spotted sea bass, *ut* protein sequences from human (*Homo sapiens*), zebrafish (*Danio rerio*), medaka (*Oryzias latipes*) and fugu (*Takifugu rubripes*) were obtained from the NCBI database. These sequences were used as queries to search the reference genome (PRJNA407434), RNA-Seq (PRJNA347604) and Iso-Seq databases (PRJNA515783) of spotted sea bass using TBLASTN with e-values of $1e^{-5}$ as threshold. The *ut* genes sequences derived from the spotted sea bass were aligned against the reference genome (PRJNA407434) to facilitate the precise determination of genomic coordinates, interval spanned, and gene length. Open reading frames were predicted using the online ORF Finder tool available at https://www.ncbi.nlm.nih.gov/orffinder/. Amino acid sequences encoded by these genes were predicted using the NCBI's ORF Finder. The validity of these sequences was ascertained by BLASTP analysis against the NCBI non-redundant protein database (NR), corroborating the accuracy of the genomic data. Additionally, the isoelectric point (pI) and molecular weight (MW) of urea transporters were determined using online ExPASy tools (http://web.expasy.org/).

2.3 Phylogenetic, Homology and Syntenic Analyses

To validate the annotation and elucidate the evolutionary relationships within the *ut* gene family of the spotted sea bass, we retrieved full-length amino acid sequences from representative higher vertebrates and teleost, including human (*Homo sapiens*), rat (*Rattus norvegicus*), mouse (*Mus musculus*), chicken (*Gallus gallus*), zebrafish (*Danio rerio*), medaka (*Oryzias latipes*), stickleback (*Gasterosteus aculeatus)*, fugu (*Fugu rubripes*), Japanese eels (*Anguilla japonica*) and large yellow croaker (*Larimichthys crocea*) from the NCBI database. These sequences were utilized to construct a phylogenetic tree. Multiple protein sequence alignments were performed using the MUSCLE software with default parameters. Subsequently, the phylogenetic tree

was generated using MEGA7.0 software, employing the neighbor-joining (NJ) method and the Jones-Taylor-Thornton (JTT) model (Jones *et al*., 1992). Bootstrap replications were set at 1000 (Kumar *et al*., 2016). Further modifications to the constructed phylogenetic tree were made using the online iTOL tool (https://itol.embl.de/login.cgi).

Homology analysis was performed to investigate the evolution relationships of *ut* genes in higher vertebrates or teleost. The *ut* genes from human, mouse, rat, chicken, zebrafish, fugu, medaka, and spotted sea bass were selected for comparison of gene distribution on chromosomes. The homology and distribution patterns were visualized using the Circos program (v0.69).

To further support the annotation and illustrate the genomic context of *ut* genes, syntenic analysis was conducted among the species mentioned above. The neighboring genes of *ut* genes in the spotted sea bass were extracted from the annotation information of the reference genome. The conserved syntenic regions of *ut* genes in other species were identified using the Genomicus (Louis *et al*., 2015) and Ensemble genome databases (http://www.ensembl.org/).

2.4 Positive Selection Analysis

The coding sequences of UT genes in several representative species (the same as those used in the phylogenetic analysis) were translated into protein sequences and aligned using the MUSCLE software (Edgar, 2004). Subsequently, the aligned protein sequences were back-translated into nucleotide-coding sequences. To assess whether the teleost UT gene family underwent adaptive sequence evolution, site, branch, and branch-site models were employed to test selection pressure using the codeml program from the PAML v4.9 package (Yang, 2007), based on the results of our phylogenetic tree. The rates of non-synonymous to synonymous substitutions (ω or dN / dS) were calculated with a priori partitions for foreground branches, as described in the PAML manual. Branches corresponding to *ut-a*, *ut-b*, and *ut-c* in the spotted sea bass were individually tested for positive selection. A likelihood ratio test (LRT) was employed to assess statistical significance. Sites under positive selection were identified using Bayesian methods (Yang *et al*., 2005).

2.5 Healthy Tissues Collection and Salinity Adaptation Experiments

Nine adult spotted sea bass specimens (average body weight: 235.75 g ± 41.87 g, average body length: 32.25 cm ± 7.26 cm) were collected from Laizhou Bay, Bohai Sea, China to examine the expression levels of *ut* mRNA in various tissues. Upon euthanasia using MS-222 (200 mg L^{-1}), eleven tissues, namely hypophysis, kidney, stomach, heart, intestine, liver, muscle, brain, skin, spleen, and gill, were promptly dissected. Subsequently, the tissues were rapidly frozen using liquid nitrogen and stored at −80℃ until RNA extraction.

Salinity transfer experiments were conducted at Dongying Shuangying Aquaculture Company, located in Shandong Province, China. Prior to the experiment, ninety individuals (average body weight: 120.66 g ± 11.87 g, average body length: 22.41 cm ± 4.26 cm) were evenly distributed into six 150 L cuboid tanks (15 fish per tank). Among them, three tanks were filled with freshwater (salinity 0) and the others with seawater (salinity 30), for a three-week acclimation period. During acclimation, salinity was precisely regulated, with water temperature at 15℃ ± 0.5℃, dissolved oxygen at (7.1 ± 0.4) mg L^{-1}, and pH at 8.0 ± 0.3. After the acclimation, fish from the seawater tanks were immediately transferred to the freshwater tanks (SF group), and fish from the freshwater tanks were transferred to the seawater tanks (FS group). Samples were collected at 0 h, 12 h, 24 h, 3 d, and 7 d post-transition. Fish were euthanized with MS-222 (200 mg L^{-1}), and gills were excised. Gill arches and filaments were dissected, rinsed in PBS to remove blood and mucus, and blotted dry with gauze. Samples were either snap-frozen in liquid nitrogen for RNA extraction at −80℃ or fixed in 4% paraformaldehyde for 24 h and stored in 70% ethanol for histological analysis. The fish health was rigorously monitored, with all specimens maintaining good health and showing no signs of abnormal behavior or physiological distress. No mortality was observed during the experiment.

2.6 RNA Extraction and Quantitative Real-Time PCR (qPCR) Analysis

The total RNA was extracted from tissue samples using TRIzol reagent (Invitrogen, CA, USA) following the manufacturer's protocol. Subsequently, the quality and concentration of the extracted RNA were assessed using a NanoDrop BD-1000 spectrophotometer (NanoDrop Technologies, Wilmington, DE, USA). RNA integrity was further evaluated through 1% agarose gel electrophoresis. Next, the RNA from each sample was reversely transcribed to cDNA using the PrimeScriptTM RT reagent kit (Takara, Otsu, Japan) according to the manufacturer's instructions. The resulting cDNA concentration was then adjusted to 500 ng μL^{-1} in preparation for subsequent qPCR experiments.

Gene-specific primers were designed using Primer 5 software and NCBI Primer-BLAST, based on the coding sequences of the UT genes in the spotted sea bass (see Table 1). The 18S rRNA of the spotted sea bass served as an internal positive control for qPCR normalization. Quantitative real-time PCR (qPCR) was conducted with 7300 machine (Applied Biosystems, CA, USA) using the SYBR Premix Ex TaqTM kit (Takara, Shiga, Japan) according to the manufacturer's instructions. The qPCR cycling conditions were as follows: initial denaturation at 95℃ for 30 s, followed by 40 cycles of denaturation at 95℃ for 5 s, annealing at the specific melting temperature (Tm) for 30 s, and extension at 72℃ for 30 s. Each reaction volume was 20 μL, comprising 2 μL (4× diluted) of cDNA template, 10 μL of SYBR premix Ex Taq, 0.4 μL of forward primer, 0.4 μL of reverse primer, 0.4 μL of ROX Reference Dye, and 6.8 μL of ddH_2O. The PCR analysis was performed in triplicate (technical replicates). The cycle threshold (Ct) values of each sample were utilized to calculate the relative expression levels using the $2^{-\Delta\Delta Ct}$ method. Statistical analysis was

conducted using one-way ANOVA followed by Duncan's multiple tests with SPSS 21.0 software (SPSS Inc., Chicago, USA). Statistical significance was considered when the $P<0.05$.

Table 1 Primers used for qPCR

Primer name	Primer sequence 5'–3' (bp)
18S-F	GGGTCCGAAGCGTTTACT
18S-R	TCACCTCTAGCGGCACAA
ut-a-F	GGCTCACCCGGACATACTG
ut-a-R	GCCACTGAGAGGGTTGTTGA
ut-b-F	GCCTCTGTCTGTGGTCTCCTA
ut-b-R	CCTCTTCTTGGCAGCGTCTT
ut-c-F	CATCATCATCGTCCTCTACC
ut-c-R	CCACGCAATACCTCCAC

2.7 Location of *ut-a* and *ut-c* in Spotted Sea Bass Gill Following Salinity Adaptation

Primers incorporating T7 and SP6 RNA polymerase sites (Table 2) were designed and employed to generate template DNA. Sense and antisense probes for *in vitro* transcription of *ut* genes were synthesized using DIG RNA labeling kits (Roche Diagnostics, Mannheim, Germany).

The gill tissue underwent dehydration (using a gradient of alcohol and xylene) following fixation in 4% paraformaldehyde for 24 h. Subsequently, the tissue was infiltrated with paraffin and embedded. Seven-micron-thick sections were then cut for *in situ* hybridization (ISH). These sections were dewaxed (treated with xylene), rehydrated (treated with a gradient of alcohol), and processed through the following solutions: 0.2 mol L^{-1} HCl (8 min), PBS (5 min, repeated twice), 10 μg mL^{-1} Proteinase K (in PBS) (37℃, 5 min), PBS (5 min), 0.1 mol L^{-1} pH 8.0 triethanolamine-HCl with 0.25% acetic anhydride (10 min), and 2X SSC (5 min). Then the sections were prehybridized at 55℃ for 1 h in probe-free hybridization buffer (composed of 50% deionized formamide, 5X SSC, 5X Denhardt's solution, 1 mg mL^{-1} yeast tRNA, and 10% dextran sodium sulfate). The probe was then diluted with hybridization buffer and allowed to hybridize in a molecular hybridization furnace at 55℃ for 16–20 h. All operations were carried out under RNase-free conditions. After hybridization, unbound probes were washed away with a series of gradient SSC solutions preheated to 55℃. Following treatment with a blocking solution, DIG-labeled probes were detected using an alkaline phosphatase-coupled anti-DIG antibody (diluted 1:3000; Roche Diagnostics), and color development was achieved using a stock solution of nitroblue tetrazolium/5-bromo-4-chloro-3-aminodiphosphate (NBT/BCIP; Roche Diagnostics, Mannheim, Germany).

Table 2 Primers used for ISH

Primer name	Primer sequence 5'–3' (bp)
ISH-*ut-a*-F	CGCATTTAGGTGACACTATAGAAGCGTGTTTGGGAAATGGATG
ISH-*ut-a*-R	CCGTAATACGACTCACTATAGGGAGACAGAATGAGGACTTGGGAGA
ISH-*ut-c*-F	CGCATTTAGGTGACACTATAGAAGCGGGGTGACCAGGGTGATT
ISH-*ut-c*-R	CCGTAATACGACTCACTATAGGGAGACAGGGAGTAGAGCAGGACAGC

3 Results

3.1 Identification of *ut* Genes in Spotted Sea Bass

In our study, three *ut* genes were identified in spotted sea bass, namely *ut-a*, *ut-b* and *ut-c*. The characteristics of three *ut* genes were summarized in Table 3. Specifically, *ut-a* was located on chr8, *ut-b* on chr17, and *ut-c* on chr23. The number of exons ranged from 5 to 10, and the length of the amino acid sequences varied from 287 to 493 aa. The molecular weights were determined to be 54.79 kDa for *ut-a*, 41.03 kDa for *ut-b*, and 30.57 kDa for *ut-c*. The predicted protein of *ut-a* exhibited an acidic isoelectric point (pI) of 5.53, while the pI values for *ut-b* and *ut-c* were alkaline, with values of 8.70 and 8.71, respectively. The sequence information of the *ut* genes in the spotted sea bass has been submitted to the GenBank database, and their accession numbers are provided in Table 3.

Table 3 Summary of *ut* genes in spotted sea bass

Gene	Position (bp)	Exon	ORF length (bp)	Protein length (aa)	Domain	MW (kDa)	pI	NCBI accession no.
ut-a	Chr8: 556112–561058	10	1479	493	UT	54.79	5.53	MT129781
ut-b	Chr17: 15924277–15927074	7	1128	376	UT	41.03	8.70	MT129782
ut-c	Chr23: 9133729–9147674	5	1218	287	UT	30.57	8.71	MT129783

3.2 Phylogenetic, Homology and Syntenic Analyses

An unrooted Neighbor-joining tree was constructed to validate the gene annotation and assess the evolutionary relationships of *ut* genes among representative species and the spotted sea bass. As depicted in Fig.1A, the phylogenetic tree was primarily categorized into 5 clades: higher vertebrate *ut-a*, higher vertebrate *ut-b*, teleost *ut-a*, teleost *ut-b*, and teleost *ut-c*. Additionally, the results indicated that *ut-a* genes and *ut-b* genes in teleost were grouped with high bootstrap support, suggesting the conservation of *ut-a* and *ut-b* genes during the evolution of teleost. Notably, as a fish-specific gene, *ut-c* genes formed a distinct clade separate from other members of the *ut* gene family. The clustering of the three *ut* genes in the spotted sea bass with their corresponding clades validated the accuracy of the classification and annotation of *ut* genes.

Homology analysis of *ut* genes was conducted to explore duplicated *ut* genes and compare their genomic distribution among selected higher vertebrates and teleost. As illustrated

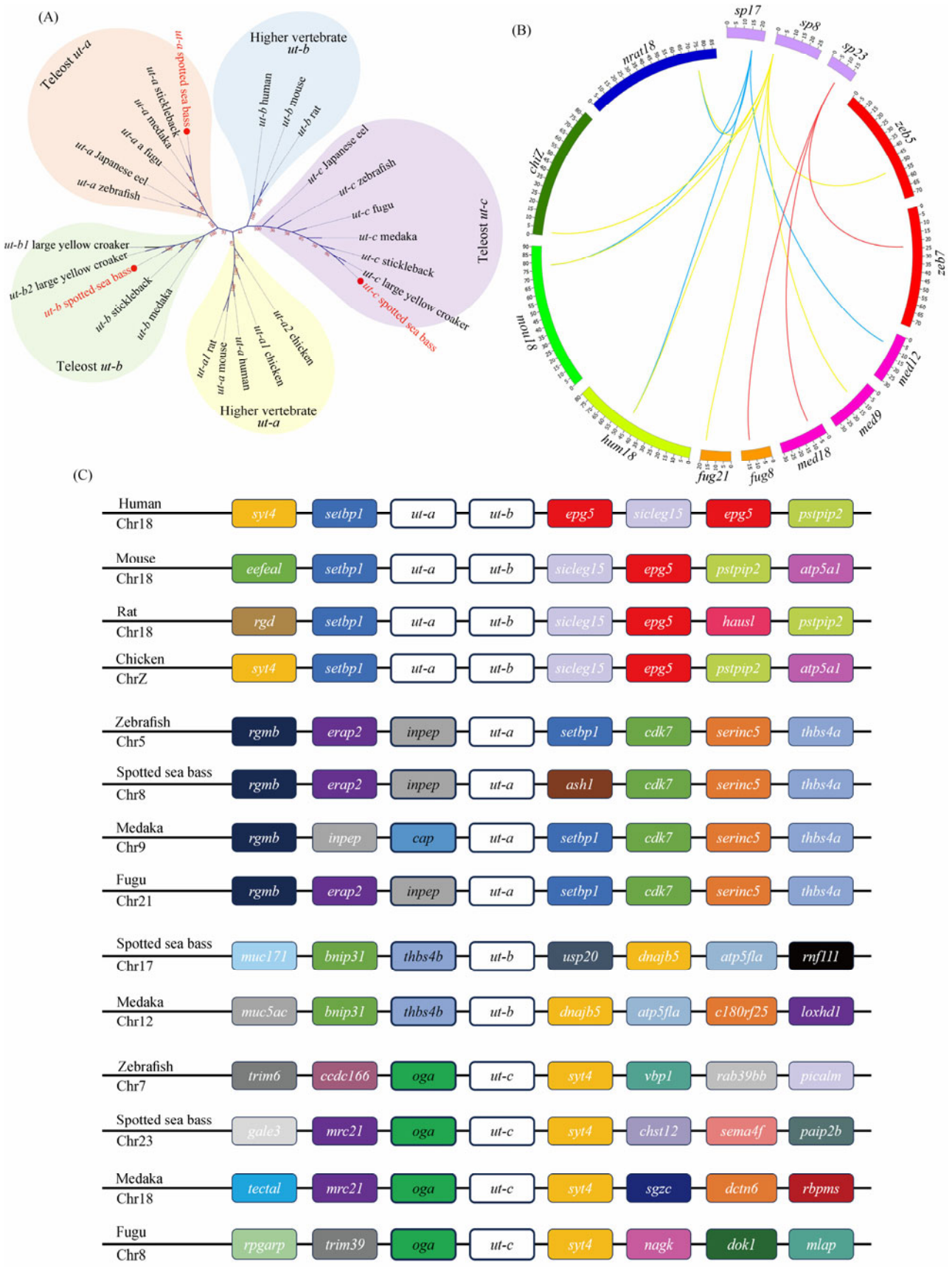

Fig.1 Identification and annotation of *ut* genes. (A) Phylogenetic tree of the *ut* gene family in representative species and spotted sea bass. Bootstrap values are indicated by text within clades. The *ut* genes of spotted sea bass are denoted by red dots and text. (B) Chromosomal distribution of orthologous *ut* genes in several vertebrates. Labels 'sp', 'zeb', 'med', 'fug', 'hum', 'mou', 'chi', and 'nrat' represent spotted sea bass, zebrafish, medaka, fugu, human, mouse, chicken, and rat, respectively. Links of the same color denote homologous genes among selected species. (C) Syntenic analysis of *ut* genes in human, mouse, rat, chicken, zebrafish, medaka, fugu, and spotted sea bass. Target *ut* genes are highlighted with white boxes.

in Fig.1B, *ut-a* and *ut-b* genes in higher vertebrates were clustered on the same chromosome. In contrast, *ut-a*, *ut-b*, and *ut-c* genes in all selected teleost were individually dispersed across distinct chromosomes.

Additionally, syntenic analysis was conducted to provide further clarification regarding the neighboring regions of *ut* genes in selected species (Fig.1C). *ut-a* and *ut-b* genes in higher vertebrates were found to be tandemly arranged with conserved syntenic blocks. In contrast, *ut* genes in teleost, which share similar genomic neighbors, were dispersed throughout the corresponding chromosomes.

3.3 Copy Number Analysis of *ut* Genes Family

The copy number of *ut* genes in representative vertebrates and the spotted sea bass is summarized in Table 4. Generally, the total number of *ut* genes varied from 2 to 3. In higher vertebrates, only two *ut* genes, *ut-a* and *ut-b*, were identified. In contrast, the tested teleost typically possess 3 *ut* genes, including *ut-a*, *ut-b*, and *ut-c*. Notably, the *ut-c* gene has not been identified in higher vertebrates, suggesting it may be a teleost-specific *ut* gene.

Table 4 the copy number of *ut* genes in spotted sea bass and several representative animals

Name	Human	Mouse	Rat	Chicken	Zebrafish	Medaka	Stickleback	Large yellow croaker	Japanese eel	Fugu	Spotted sea bass
ut-a	1	1	1	0	1	1	1	0	1	1	1
ut-b	1	1	1	2	0	1	1	2	0	0	1
ut-c	0	0	0	0	1	1	1	1	1	1	1
Total	2	2	2	2	2	3	3	3	2	2	3

3.4 Positive Selection Detection of *ut* Genes in Spotted Sea Bass

To gain a deeper understanding of the evolution of *ut-a*, *ut-b*, and *ut-c* genes in spotted sea bass, selection pressure analysis was conducted using site, branch, and branch-site models within the codeml program. Initially, three pairs of site models were employed to identify the evolutionary forces acting on individual codon sites (Tables 5–7), including M1 (neutral) *vs*. M2 (selection), M0 (one ratio) *vs*. M3 (discrete), and M7 (beta) *vs*. M8 (beta and ω). The results of the M3 *vs*. M0 comparison indicated heterogeneity in the ω ratio among codon sites of *ut-a*, *ut-b*, and *ut-c*. Furthermore, the selection M8 model significantly outperformed the neutral M7 model, suggesting that *ut-a*, *ut-b*, and *ut-c* were subject to positive selection.

Table 5 Site model for the selective pressure analysis of *ut-a* genes

Model	ln*L*	np	Model compared	$2^{\triangle}\ln L$	d.f.	*P*-value	Positive selected sites
M0 (one ratio)	−6757.607062	15					
M1 (nearly neutral)	−6531.469279	16					Not allowed
M2 (positive selection)	−6531.469279	18	M2 *vs*. M1	0	2	1.00	
M3 (discrete)	−6485.901531	19	M3 *vs*. M0	543.411	4	1.00×10^{-9}	
M7 (beta)	−6501.188259	16					Not allowed
M8 (beta and ω)	−6486.328919	18	M8 *vs*. M7	29.719	2	3.52×10^{-7}	

Table 6 Site model for the selective pressure analysis of *ut-b* genes

Model	ln*L*	np	Model compared	$2^{\triangle}\ln L$	d.f.	*P*-value	Positive selected sites
M0 (one ratio)	−4841.974090	13					
M1 (nearly neutral)	−4767.915085	14					Not allowed
M2 (positive selection)	−4767.535030	16	M2 *vs*. M1	0.760	2	0.68	
M3 (discrete)	−4755.216480	17	M3 *vs*. M0	173.515	4	1.00×10^{-9}	
M7 (beta)	−4763.359858	14					Not allowed
M8 (beta and ω)	−4756.363787	16	M8 *vs*. M7	13.992	2	9.16×10^{-4}	

Table 7 Site model for the selective pressure analysis of *ut-c* genes

Model	ln*L*	np	Model compared	$2^{\triangle}\ln L$	d.f.	*P*-value	Positive selected sites
M0 (one ratio)	−4560.654166	13					
M1 (nearly neutral)	−4499.213502	14					Not allowed
M2 (positive selection)	−4499.213502	16	M2 *vs*. M1	0	2	1.00	
M3 (discrete)	−4488.618021	17	M3 *vs*. M0	144.072	4	1.00×10^{-9}	
M7 (beta)	−4492.114566	14					Not allowed
M8 (beta and ω)	−4488.648962	16	M8 *vs*. M7	6.931	2	0.03	

Branch and branch-site models were also utilized to investigate whether *ut* genes of the spotted sea bass lineage evolved under different positive selection pressures relative to other lineages. Three unrooted Neighbor-Joining trees of *ut-a*, *ut-b*, and *ut-c* were respectively constructed for their selection pressure analyses (Fig.2). The results of branch and branch-site models indicated that the branches of *ut-b* and *ut-c* in spotted sea bass were significantly influenced by positive selection, as shown in Tables 8–9. Additionally, several positively selected sites of *ut-b* and *ut-c* genes were identified in the branch-site model using Bayes empirical Bayes (BEB) with a posterior probability exceeding 95%,

as show in Table 9. These positively selected sites were identified as 103 C, 169 L, 265 A, 270 G, 274 L, 277 H, 278 R, and 284 V. Detailed information is provided in Table 9.

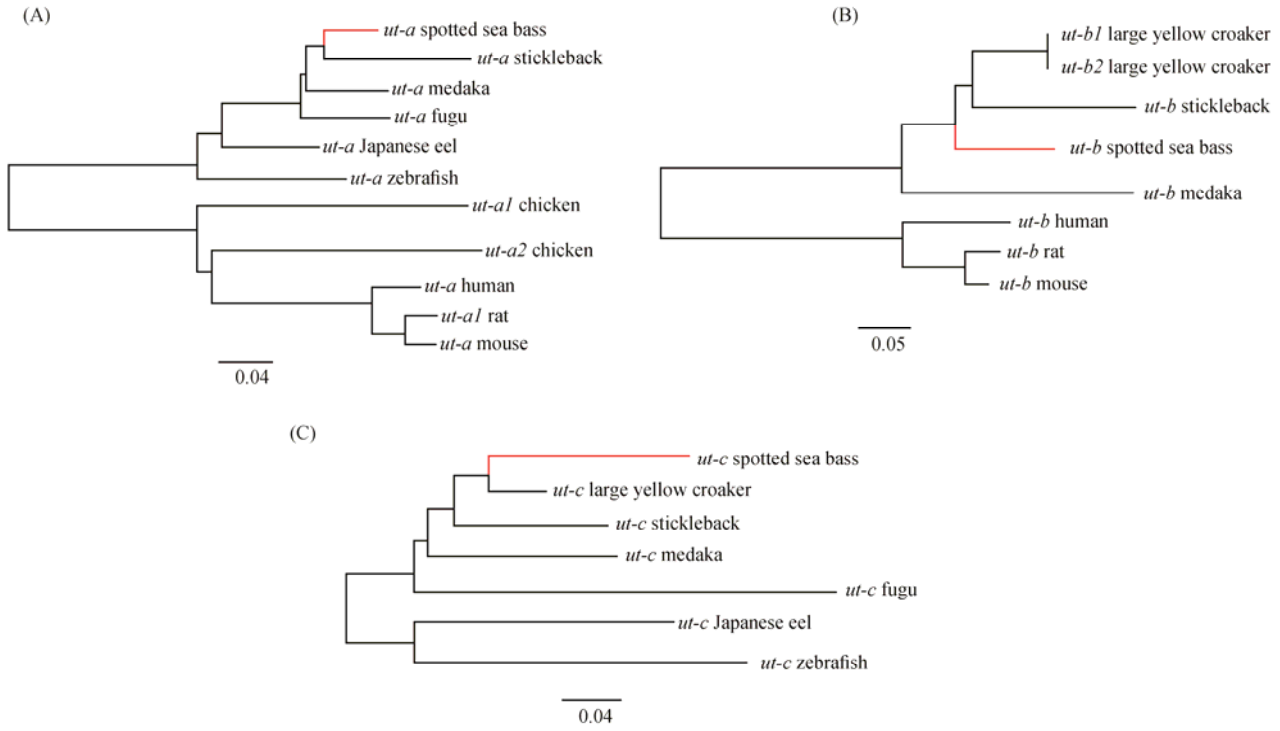

Fig.2 Positive selection detection of *ut-a* (A), *ut-b* (B) and *ut-c* (C) in spotted sea bass using branch and branch-site model. Branch with red color indicated the foreground branch in the branch and branch-site models.

Table 8 Branch model for the positive pressure analysis of *ut-a*, *ut-b* and *ut-c* genes in spotted sea bass

Model		ln*L*	np	Model compared	$2^{\triangle}$ln*L*	d.f.	*P*-value
Branch model for *ut-a*	M0	−6757.607062	15				
	M2	−6756.649358	16	M2 *vs*. M0	1.915	1	0.17
Branch model for *ut-b*	M0	−4841.974090	13				
	M2	−4837.164873	14	M2 *vs*. M0	9.618	1	1.93×10^{-3}
Branch model for *ut-c*	M0	−4560.654166	13				
	M2	−4552.756663	14	M2 *vs*. M0	15.795	1	7.06×10^{-5}

Table 9 Branch-site model for the positive pressure analysis of *ut-a*, *ut-b* and *ut-c* genes in spotted sea bass

Model		ln*L*	np	Model compared	$2^{\triangle}$ln*L*	d.f.	*P*-value	Positive selected sites
Branch-site model for *ut-a*	Null Model A	−6530.370156	17					
	Model A	−6528.459733	18	Model A *vs*. Model A null	3.821	1	0.05	
Branch-site model for *ut-b*	Null Model A	−4767.801249	15					
	Model A	−4755.983766	16	Model A *vs*. Model A null	23.635	1	1.17×10^{-6}	169 L (0.992)
Branch-site model for *ut-c*	Null Model A	−4487.991610	15					
	Model A	−4462.421728	16	Model A *vs*. Model A null	51.140	1	1×10^{-9}	103 C (0.996) 265 A (0.997) 277 H (0.989) 270 G (0.993) 274 L (0.996) 278 R (0.999) 284 V (0.992)

3.5 Tissue-Specific Expression Analysis of *ut* Genes

Expression patterns of genes are correlated with their biological functions. To gain insight into the tissue-specific expression patterns of *ut* genes in spotted sea bass, quantitative real-time PCR (qPCR) was performed to assess the expression of *ut* genes in 11 tissues. As depicted in Fig.3, *ut* genes exhibited ubiquitous expression and distinct tissue-specific expression patterns in spotted sea bass. Specifically, *ut-a* was found to be highly expressed in the gill com-

pared to other tissues (Fig.3A), *ut-b* showed predominant expression in the spleen, heart, and brain, followed by the kidney, skin, and gill (Fig.3B). The highest expression levels of *ut-c* were observed in the kidney (Fig.3C).

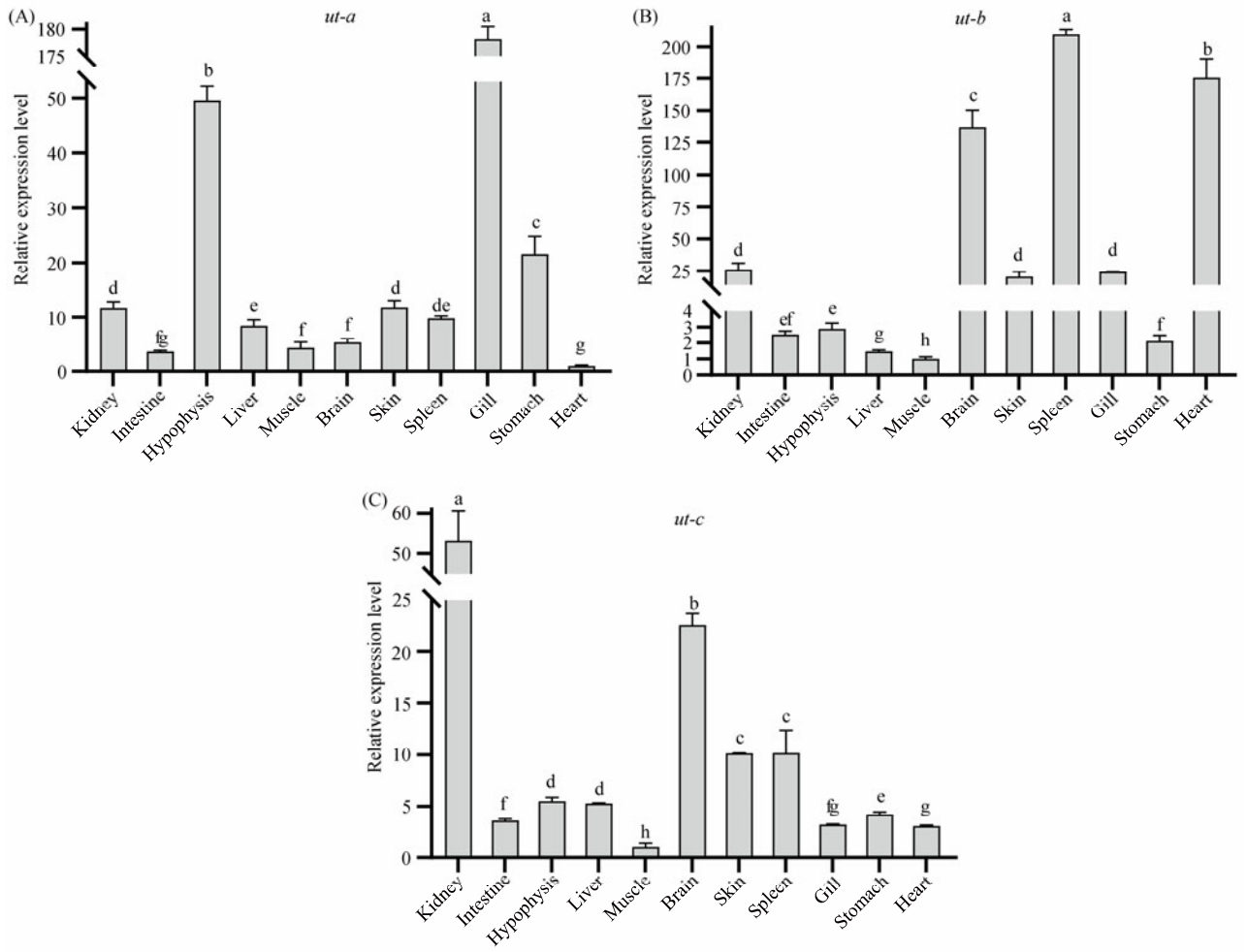

Fig.3 Expression patterns of 3 *ut* genes in healthy tissues of spotted sea bass. Different letters above bars represented significant difference ($P<0.05$).

3.6 Expression Analysis of *ut* Genes During Freshwater and Seawater Adaptation

To investigate the potential roles of *ut* genes during freshwater and seawater adaptation in teleost, quantitative real time PCR (qPCR) analysis was employed to determine the expression patterns of three *ut* genes in osmoregulation-related tissues, specifically the gill and kidney of spotted sea bass, at 0 h, 12 h, 24 h, 3 d, and 7 d after the fish were transfered from freshwater to seawater and from seawater to freshwater. Overall, all three *ut* genes exhibited salinity-related expression patterns in both gill and kidney.

As depicted in Fig.4A, a notable repression in the expression of the *ut-a* gene was observed in the gill of spotted sea bass during freshwater to seawater (FS) adaptation. Conversely, during the seawater to freashwater (SF) adaptation, expression levels of the *ut-a* gene were significantly up-regulated from 24 h to 3 d in the gill (Fig.4C). In the kidney, *ut-a* displayed significantly up-regulated expression patterns during both FS and SF adaptation (Figs.4B and D).

The expression of the *ut-b* gene was markedly suppressed in both gill and kidney tissues during both SF and FS adaptation, as shown in Fig.4A. Regarding the *ut-c* gene, it exhibited significant induction in the gill from 12 h to 7 d after the fish were transferred to seawater (Fig.4A). However, during SF adaptation, the expression levels of *ut-c* gene were dramatically suppressed, particularly at 24 h, 3 d, and 7 d (Fig.4C). In the kidney, the expression levels of the *ut-c* gene were significantly increased from 12 h to 7 d after the fish were transferred to seawater (Fig.4B). Notably, in the kidney, *ut-c* genes displayed a significant expression change only at 24 h after the fish were transferred to seawater (Fig. 4D).

3.7 Localization of *ut-a* and *ut-c* in Gills

In situ hybridization was employed to localize the *ut-a* and *ut-c* genes to investigate differences in their expression distribution in gill tissues during FS adaptation. The results of *in situ* hybridization are illustrated in Fig.5. During FS adaptation, the signals of *ut-a* in the gills were evenly distributed throughout the epithelial cells of the gill lamellae, including the top, middle, and bottom regions, as well as in the epithelial cells of the gill filaments between adjacent gill

lamellae (Figs.5A, B, and C). Signals of the *ut-c* gene were primarily observed at 7 days of FS adaptation, concentrated at the bottom of the gill lamellae and in the epithelial cells of the gill filaments between adjacent gill lamellae (Fig.5E).

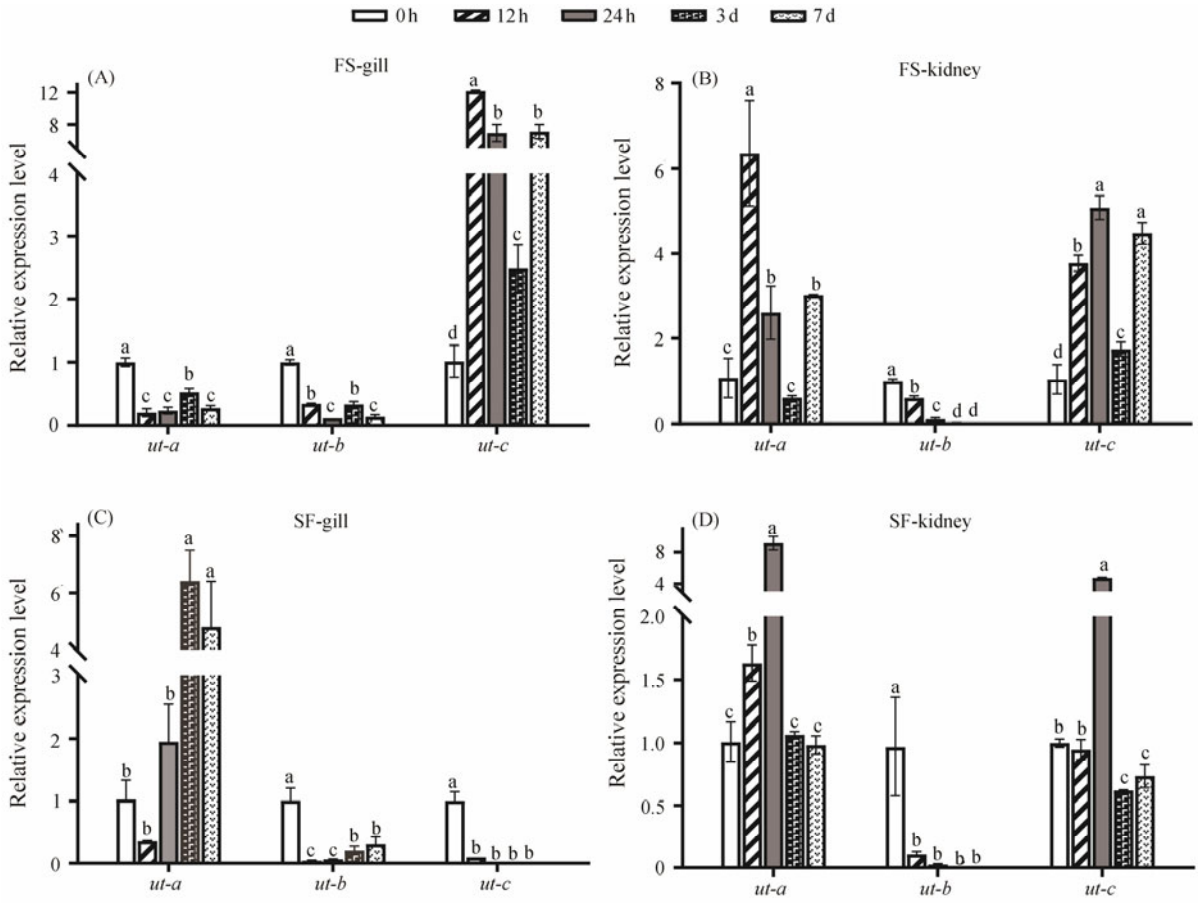

Fig.4 Expression patterns of *ut* gene family in the gill, kidney at 0 h, 12 h, 24 h, 3 d and 7 d after salinity transfer. FS represents group transferred from freshwater to seawater, and SF represents group transferred from seawater to freshwater. Various letters among same gene represented significant difference ($P<0.05$).

4 Discussion

In this study, three *ut* genes were identified in the spotted sea bass from genomic databases. Phylogenetic analysis revealed that *ut-c* genes formed a distinct clade separate from other members of the *ut* gene family, consistent with findings in other teleost species (Abinash *et al*., 2005). Additionally, no conserved syntenic relationships or regions were observed between *ut* genes in selected higher vertebrates and teleost, suggesting distinct evolutionary processes for *ut* genes. Branch-site models were used in our study, which are useful for identifying positive selection along prespecified lineages that affect only a few sites in the protein (Yang and Nielsen, 2002). By employing branch-site models, we identified positive selection acting on *ut* genes during evolution. Specifically, eight positive selection sites were identified, likely contributing to functional divergence. Interestingly, most positive selection sites in *ut-c* gene were located within its functional UT domain (11–267 aa), potentially impacting the urea transport capability of *ut-c* in the spotted sea bass. Our findings underscore the significant role of positive selection in shaping the evolution of the *ut* gene family, with positively selected amino acid sites potentially driving functional divergence among species.

Expression profiling of *ut* genes across different tissues provided insights into their potential functions. The *ut* genes exhibited unique tissue-specific expression patterns, with *ut-c* showing the highest expression levels in the kidney (Fig.3C). This finding is consistent with previous observations in Japanese eels (Abinash *et al*., 2005), gulf toadfish (*Opsanus beta*) and spiny dogfish shark (Wood *et al*., 1995), where *ut* genes were highly expressed in the gill and/or kidney, key tissues involved in ammonia excretion in fish (Wood*et al*., 1995; Smith and Wright, 1999; McDonald *et al*., 2006). Additionally, a relatively high expression level of the *ut-c* gene was observed in the brain, suggesting a potential role in preventing urea diffusion from the osmotically active plasma into cellular compartments, thereby maintaining the stability of the brain cell microenvironment. This observation aligns with previous reports of prominent expression of urea transporters in the brains of mammals and elasmobranchs, such as rats and spiny dogfish shark (Couriaud *et al*., 1996; Smith and Wright, 1999). Studies by Frame and Cumming (2022) have further highlighted the role of astrocytes in scavenging toxic ammonia through the

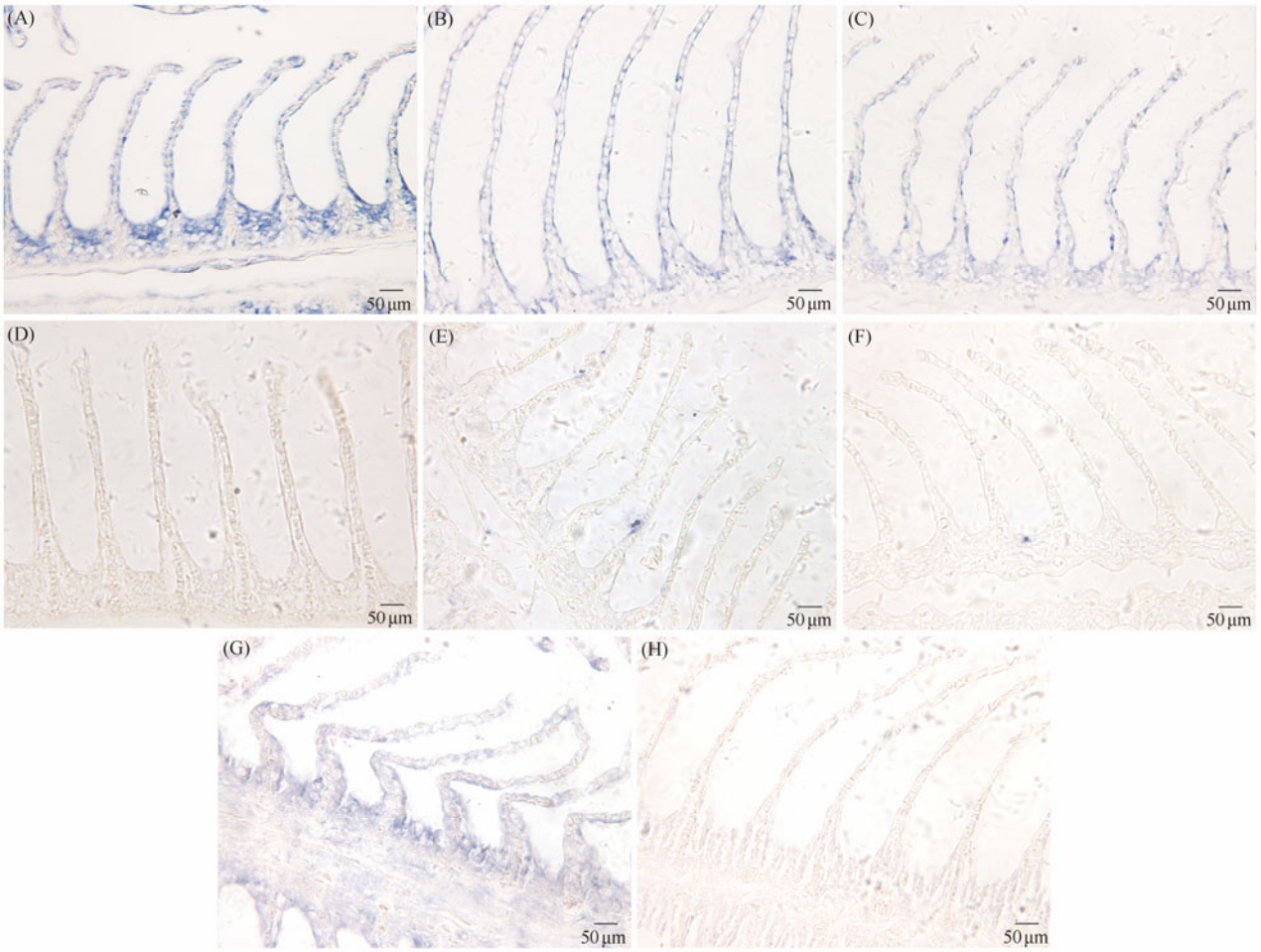

Fig.5 *ut-a* and *ut-c* mRNA in the gill of spotted sea bass was detected by *in situ* hybridization (ISH). (A)–(D) Positive signals of *ut-a* mRNA in the gills of spotted sea bass at FS adaptation for 0 d (A), 3 d (B), and 7 d (C), while negative signals shown in (D). (E)–(H) Positive signals of *ut-c* mRNA in the gills of spotted sea bass at FS adaptation for 0 d (E), 3 d (F), and 7 d (G), while negative signals shown in (H). The blue dot in Figs.(A)–(C) is positive signal of *ut-a* gene. The blue dot in Figs. (E)–(G) is positive signal of *ut-c* gene.

urea cycle, thereby protecting brain tissue.

Previous studies have shown an increase of cortisol expression during salinity acclimatization (Evans *et al*., 2005). Cortisol has been detected to stimulate gluconeogenesis and proteolysis in fish, leading to elevated plasma ammonia levels. The glucocorticoid-mediated increase in urea synthesis may thus serve as a mechanism for ammonia detoxification (McDonald *et al*., 2004). Consequently, the up-regulation of *ut-a* expression during seawater or freshwater adaptation may facilitate the excretion of excess urea generated under stress (McDonald *et al*., 2006). However, the mechanisms underlying this process remain poorly understood, highlighting the need for further research in this area.

The expression of the *ut-b* gene was significantly suppressed in both gill and kidney tissues during freshwater-seawater and seawater-freshwater adaptation, as shown in Fig.4. These findings suggest that the capacity for urea transport mediated by *ut-b* may be severely impaired during salinity adaptation in spotted sea bass. Furthermore, despite the close evolutionary relationship observed between *ut-a* and *ut-b* genes in sequence analysis and phylogenetic tree construction, they exhibited distinct expression patterns in response to salinity adaptation. This discrepancy implies inherent differences in their responses to salinity adaptation in spotted sea bass.

In the kidney, the expression levels of the *ut-c* gene significantly increased from 12 h to 7 d after fish were transferred to seawater (Fig.4B). Previous studies in teleost have proved the function of *ut-c* gene in stimulating urea reabsorption to counterbalance the osmotic stress of the aquatic environment (Mistry *et al.*, 2001, 2005). This likely accounts for the observed differential expression of the *ut-c* gene following fish transfers. Up- or down-regulation of *ut-c* expression may enhance or weaken urea reabsorption, respectively, thereby helping to maintain tissue osmolality (Mathai, 2005). Similar findings have been reported in the Japanese eel, where *ut-c* gene expression significantly increased in the kidney following transfers from freshwater to seawater (Mistry *et al*., 2005).

In this study, we observed the expression distribution of *ut-a* and *ut-c* genes during the adaptation from freshwater to seawater in spotted sea bass by *in situ* hybridization. During freshwater adaptation, the *ut-a* gene expression was uniformly observed across the epithelial cells of the gill lamel-

lae, encompassing the apical, medial, and basal regions, as well as within the epithelial cells of the gill filaments interposed between contiguous gill lamellae. The ubiquitous expression profile of the *ut-a* gene implies a fundamental role in sustaining the physiological integrity of gill tissue and in contributing to a spectrum of physiological processes. In contrast, the *ut-c* gene signal predominantly localized to the gill lamellae epithelial cells situated between the gill base and neighboring gill lamellae following a 7-d saline adaptation period. This delayed and localized expression pattern of the *ut-c* gene suggests its critical role in the later stages of salinity adaptation, potentially linked to the specific physiological requirements for coping with high-salinity environments.

In summary, our study identified and characterized all three *ut* genes, namely *ut-a*, *ut-b* and *ut-c*, in the spotted sea bass. Through phylogenetic, homology, and syntenic analyses, we confirmed their annotation and evaluated their evolutionary relationships among higher vertebrates, teleost, and spotted sea bass. Selection pressure analyses suggest that positive selection likely play a significant role in the evolution of the *ut* gene family, with positively selected amino acid sites potentially contributing to functional divergence among species. Additionally, tissue-specific expression patterns were observed, with prominent expression in gill and kidney tissues. Furthermore, all three *ut* genes exhibited salinity-related expression patterns in the gill and kidney tissues during freshwater and seawater adaptation, indicating their physiological importance even in ammonotelic teleost fishes. Overall, our findings contribute to a deeper understanding of the evolutionary relationships and physiological significance of urea transporters in teleost.

Acknowledgements

This research was supported by the National Natural Science Foundation of China (No. 32072947), and the China Agriculture Research System (No. CARS-47).

Author Contributions

Conceptualization: Rutao Yang, Zurui Huang, Yun Li; Methodology: Rutao Yang, Zurui Huang, Jinku Li, Xin Qi; Validation: Rutao Yang, Zurui Huang, Jinku Li, Kaiqiang Zhang; Formal analysis: Rutao Yang, Zurui Huang; Investigation: Rutao Yang, Zurui Huang, Kaiqiang Zhang, Jinku Li; Writing-original draft preparation: Rutao Yang, Zurui Huang; Writing-review and editing: Rutao Yang, Jingru Zhang, Mengqun Liu; Supervision: Haishen Wen, Jifang Li, Meizhao Zhang; Project administration: Yun Li, Xin Qi, Haishen Wen; Funding acquisition: Yun Li, Haishen Wen. All authors have read and agreed to the published version of the manuscript.

Data Availability

The data and references presented in this study are available from the corresponding author upon reasonable request.

Declarations

Ethics Approval and Consent to Participate

All experimental spotted sea bass were housed and treated in accordance with the guidelines of the Animal Research and Ethics Committees of Ocean University of China. The ethics committee approval number is 2021092502.

Consent for Publication

Informed consent for publication was obtained from all participants.

Conflict of Interests

The authors declare that they have no conflict of interests.

References

Cabrera, D. M., Janech, M. G., Morinelli, T. A., and Miller, D. H., 2003. A thromboxane A(2) system in the Atlantic stingray, *Dasyatis Sabina*. *General and Comparative Endocrinology*, **130** (2): 157-164, https://doi.org/10.1016/s0016-6480(02)00586-5.

Couriaud, C., Leroy, C., Simon, M., Silberstein, C., Bailly, P., Ripoche, P., *et al*., 1999. Molecular and functional characterization of an amphibian urea transporter. *Biochimica et Biophysica Acta*, **1421** (2): 347-352, https://doi.org/10.1016/s0005-2736(99)00147-9.

Couriaud, C., Ripoche, P., and Rousselet, G., 1996. Cloning and functional characterization of a rat urea transporter: Expression in the brain. *Biochimica et Biophysica Acta*, **1309** (3): 197-199, https://doi.org/10.1016/s0167-4781(96)00172-8.

Edgar, R. C., 2004. MUSCLE: Multiple sequence alignment with high accuracy and high throughput. *Nucleic Acids Research*, **32** (5): 1792-1797, https://doi.org/10.1093/nar/gkh340.

Evans, D. H., Piermarini, P. M., and Choe, K. P., 2005. The multifunctional fish gill: Dominant site of gas exchange, osmoregulation, acid-base regulation, and excretion of nitrogenous waste. *Physiological Reviews*, **85** (1): 97-177, https://doi.org/10.1152/physrev.00050.2003.

Fenton, R. A., 2008. Urea transporters and renal function: Lessons from knockout mice. *Current Opinion in Nephrology and Hypertension*, **17** (5): 513-518, https://doi.org/10.1097/MNH.0b013e3283050969.

Frame, A. K., and Cumming, R. C., 2022. Using the urea cycle to shift astrocytes from harmful to helpful in Alzheimer's disease. *Cell Metabolism*, **34** (8): 1079-1081, https://doi.org/10.1016/j.cmet.2022.07.001.

Griffith, R. W., 1991. Guppies, toadfish, lungfish, coelacanths and frogs: A scenario for the evolution of urea retention in fishes. *Environmental Biology of Fishes*, **32** (1): 199-218, https://doi.org/10.1007/BF00007454.

Hyodo, S., Katoh, F., Kaneko, T., and Takei, Y., 2004. A facilitative urea transporter is localized in the renal collecting tubule of the dogfish *Triakis scyllia*. *The Journal of Experimental Biology*, **207** (Pt 2): 347-356, https://doi.org/10.1242/jeb.00773.

Jones, D. T., Taylor, W. R., and Thornton, J. M., 1992. The rapid generation of mutation data matrices from protein sequences. *Computer Applications in the Biosciences: CABIOS*, **8** (3): 275-282, https://doi.org/10.1093/bioinformatics/8.3.275.

Kakumura, K., Watanabe, S., Bell, J. D., Donald, J. A., Toop, T., Kaneko, T., *et al*., 2009. Multiple urea transporter proteins in the kidney of holocephalan elephant fish (*Callorhinchus Milii*). *Comparative Biochemistry and Physiology. Part B, Biochemistry & Molecular Biology*, **154** (2): 239-247, https://doi.org/10.1016/j.cbpb.2009.06.009.

Komrakova, M., Blaschke, M., Ponce, M. L., Klüver, A., Köpp, R., Hüfner, M., *et al*., 2020. Decreased expression of the human urea transporter *SLC14A1* in bone is induced by cytokines and stimulates adipogenesis of mesenchymal progenitor cells. *Experimental and Clinical Endocrinology & Diabetes: Official Journal, German Society of Endocrinology [and] German Diabetes Association*, **128** (9): 582-595, https://doi.org/10.1055/a-1084-3888.

Konno, N., Hyodo, S., Matsuda, K., and Uchiyama, M., 2006. Effect of osmotic stress on expression of a putative facilitative urea transporter in the kidney and urinary bladder of the marine toad, *Bufo marinus*. *The Journal of Experimental Biology*, **209** (Pt 7): 1207-1216, https://doi.org/10.1242/jeb.02123.

Kumar, S., Stecher, G., and Tamura, K., 2016. MEGA7: Molecular evolutionary genetics analysis version 7.0 for bigger datasets. *Molecular Biology and Evolution*, **33** (7): 1870-1874, https://doi.org/10.1093/molbev/msw054.

Laurent, P., Wood, C. M., Wang, Y., Perry, S. F., Gilmour, K. M., Part, P., *et al*., 2001. Intracellular vesicular trafficking in the gill epithelium of urea-excreting fish. *Cell and Tissue Research*, **303** (2): 197-210, https://doi.org/10.1007/s004410000312.

Louis, A., Nguyen, N. T., Muffato, M., and Crollius, H. R., 2015. Genomicus update 2015: KaryoView and MatrixView provide a genome-wide perspective to multispecies comparative genomics. *Nucleic Acids Research*, **43** (Database issue): D682-689, https://doi.org/10.1093/nar/gku1112.

Mathai, J. C., 2005. Ammonotelic teleosts and urea transporters. *American Journal of Physiology. Renal Physiology*, **288** (3): F453-454, https://doi.org/10.1152/ajprenal.00391.2004.

McDonald, M. D., Smith, C. P., and Walsh, P. J., 2006. The physiology and evolution of urea transport in fishes. *The Journal of Membrane Biology*, **212** (2): 93-107, https://doi.org/10.1007/s00232-006-0869-5.

McDonald, M. D., Wood, C. M., Grosell, M., and Walsh, P. J., 2004. Glucocorticoid receptors are involved in the regulation of pulsatile urea excretion in toadfish. *Journal of Comparative Physiology. B, Biochemical, Systemic, and Environmental Physiology*, **174** (8): 649-58, https://doi.org/10.1007/s00360-004-0456-y.

Mistry, A. C., Chen, G., Kato, A., Nag, K., Sands, J. M., and Hirose, S., 2005. A novel type of urea transporter, *UT-C*, is highly expressed in proximal tubule of seawater eel kidney. *American Journal of Physiology. Renal Physiology*, **288** (3): F455-465, https://doi.org/10.1152/ajprenal.00296.2004.

Mistry, A. C., Honda, S., Hirata, T., Kato, A., and Hirose, S., 2001. Eel urea transporter is localized to chloride cells and is salinity dependent. *American Journal of Physiology. Regulatory, Integrative and Comparative Physiology*, **281** (5): R1594-1604, https://doi.org/10.1152/ajpregu.2001.281.5.R1594.

Pilley, C. M., and Wright, P. A., 2000. The mechanisms of urea transport by early life stages of rainbow trout (*Oncorhynchus mykiss*). *Journal of Experimental Biology*, **203** (20): 3199-3207, https://doi.org/10.1242/jeb.203.20.3199.

Sands, J. M., 1999. Regulation of renal urea transporters. *Journal of the American Society of Nephrology*, **10** (3): 635-646, https://doi.org/10.1681/ASN.V103635.

Smith, C. P., and Wright, P. A., 1999. Molecular characterization of an elasmobranch urea transporter. *The American Journal of Physiology*, **276** (2): R622-626, https://doi.org/10.1152/ajpregu.1999.276.2.R622.

Stewart, G. S., Graham, C., Cattell, S., Smith, T. P. L., Simmons, N. L., and Smith, C. P., 2005. *UT-B* is expressed in bovine rumen: Potential role in ruminal urea transport. *AJP: Regulatory, Integrative and Comparative Physiology*, **289** (2): R605-612, https://doi.org/10.1152/ajpregu.00127.2005.

Tian, Y., Wen, H. S., Qi, X., Zhang, X. Y., and Li, Y., 2019. Identification of mapk gene family in *Lateolabrax Maculatus* and their expression profiles in response to hypoxia and salinity challenges. *Gene*, **684**: 20-29, https://doi.org/10.1016/j.gene.2018.10.033.

Uchiyama, M., Kikuchi, R., Konno, N., Wakasugi, T., and Matsuda, K., 2009. Localization and regulation of a facilitative urea transporter in the kidney of the red-eared slider turtle (*Trachemys scripta elegans*). *Journal of Experimental Biology*, **212** (2): 249-56, https://doi.org/10.1242/jeb.019703.

Walsh, P. J., Grosell, M., Goss, G. G., Bergman, H. L., Bergman, A. N., Wilson, P., *et al*., 2001. Physiological and molecular characterization of urea transport by the gills of the lake magadi tilapia (*Alcolapia grahami*). *The Journal of Experimental Biology*, **204** (Pt 3): 509-520, https://doi.org/10.1242/jeb.204.3.509.

Walsh, P. J., Heitz, M. J., Campbell, C. E., Cooper, G. J., Medina, M., Wang, Y. S., *et al*., 2000. Molecular characterization of a urea transporter in the gill of the gulf toadfish (*Opsanus beta*). *The Journal of Experimental Biology*, **203** (Pt 15): 2357-2364, https://doi.org/10.1242/jeb.203.15.2357.

Wood, C., Part, P., and Wright, P., 1995. Ammonia and urea metabolism in relation to gill function and acid-base balance in a marine elasmobranch, the spiny dogfish (*Squalus acanthias*). *The Journal of Experimental Biology*, **198** (Pt 7): 1545-1558, https://doi.org/10.1242/jeb.198.7.1545.

Wright, P., Felskie, A., and Anderson, P., 1995. Induction of ornithine-urea cycle enzymes and nitrogen metabolism and excretion in rainbow trout (*Oncorhynchus mykiss*) during early life stages. *Journal of Experimental Biology*, **198** (1): 127-135, https://doi.org/10.1242/jeb.198.1.127.

Yamaguchi, Y., Takaki, S., and Hyodo, S., 2009. Subcellular distribution of urea transporter in the collecting tubule of shark kidney is dependent on environmental salinity. *Journal of Experimental Zoology. Part A, Ecological Genetics and Physiology*, **311** (9): 705-718, https://doi.org/10.1002/jez.558.

Yang, Z., 2007. PAML 4: Phylogenetic analysis by maximum likelihood. *Molecular Biology and Evolution*, **24** (8): 1586-1591, https://doi.org/10.1093/molbev/msm088.

Yang, Z., and Nielsen, R., 2002. Codon-substitution models for detecting molecular adaptation at individual sites along specific lineages. *Molecular Biology and Evolution*, **19** (6): 908-917, https://doi.org/10.1093/oxfordjournals.molbev.a004148.

Yang, Z., Wong, W. S., and Nielsen, R., 2005. Bayes empirical bayes inference of amino acid sites under positive selection. *Molecular Biology and Evolution*, **22** (4): 1107-1118, https://doi.org/10.1093/molbev/msi097.

You, G., Smith, C. P., Kanai, Y., Lee, W. S., Stelzner, M., and Hediger, M. A., 1993. Cloning and characterization of the vasopressin-regulated urea transporter. *Nature*, **365** (6449): 844-847, https://doi.org/10.1038/365844a0.

(Edited by Qiu Yantao)